# Laser-based proton acceleration on ultra-thin foil with a 100 TW class high intensity laser system

S. Fourmaux[a], S. Buffechoux[a,b], S. Gnedyuk[a], B. Albertazzi[a,b], D. Capelli[b], L. Lecherbourg[c], A. Lévy[b], P. Audebert[b], D. Houde[d], R. Marjoribanks[c], F. Martin[a], H. Pépin[a], J. Fuchs[b] and J. C. Kieffer[a]

a INRS-EMT, Université du Québec, 1650 Lionel Boulet, Varennes J3X 1S2, Québec, Canada;
b LULI, UMR 7605, CNRS - CEA - Université Paris 6 - Ecole Polytechnique, Palaiseau, France;
c Dept. of Physics and Institute for Optical Sciences, University of Toronto, Canada;
d Université de Sherbrooke, Dép. Medecine nucléaire et radiobiologie, Fleurimont J1H 5N4, Canada

## ABSTRACT

Focusing a high intensity laser pulse, onto a thin foil target generates a plasma and energetic proton and ion beams from the target rear and front sides, propagating along the target normal. Such laser produced collimated and energetic protons beams are of high interest because of the wide range of applications: ion based fast ignitor schemes, probing of electromagnetic fields in plasma, isotopes production or hadron therapy. The 100 TW class laser system at the Advanced Laser Light Source facility, is used with an intensity close to $10^{19}$ W/cm$^2$, to study protons acceleration with femtosecond laser pulses, ultra thin foil target and high contrast laser pulse ratio. To characterize the plasma expansion, we monitor it with an imaging technique using a femtosecond laser probe. In this configuration we were able to reach a proton critical energy of 12 MeV and to work with target foil thickness as small as 15 nm.

**Keywords:** High intensity laser system, Laser plasma interaction, Laser based ions source, High contrast ratio laser pulses

## 1. INTRODUCTION

Focusing a high intensity laser pulse onto a thin foil target (a few 10's of μm or lower) generates a plasma and an energetic proton and ion beam on the target rear side along the normal axis to its surface. Such collimated and energetic protons beams production using high intensity and ultrashort laser systems have first been demonstrated in 2000 at the Lawrence Livermore National Laboratory NOVA laser [1] and at the Rutherford Appleton Laboratory VULCAN laser [2,3].

In this interaction regime the dominant acceleration mechanism is the Target Normal Sheat Acceleration (TNSA). First, electrons are accelerated by the high intensity laser on the target front side and can propagate through the target at relativistic speed. Those hot electrons can generate a strong electric field on the target rear side which can reach up to $10^{12}$ V/m. In a second step, under the action of this high quasi-static field, protons originated from hydrogenated contaminant are accelerated normal to the iso-potentials. This results in a high quality beam, accelerated normal to the target surface.

This laser based proton acceleration is producing a compact source as this mechanism occurs over ~10 μm space scale. The proton spectrum is continuous and is exponentially decreasing until a cut-off energy. Up to now the maximum reported energy was 65 MeV with 80 J energy and 600 fs laser pulse duration with a low 45 minutes shot cycle laser system [4]. The experimental results show a high current proton beam, from $10^6$ to $10^{12}$ protons per MeV per pulse, depending mainly on the laser energy, and exhibit conversion efficiency close to 1%. The obtained proton beam is highly laminar with an equivalent source point of around 4 μm and has a divergence half angle close to 15°. Such good properties allow to reach a very low emittance below 0.015 mm.rad which is well adapted for accelerator injection. The last interesting property is that the ion bunch duration is as short as several ps which make it suitable for ultrafast pump and probe schemes.

Recent published scaling laws [5] show a linear dependence of the maximum proton energy as a function of the intensity I for high intensity and high repetition rate Ti:Sapphire laser system which exhibits small pulse duration (around 50 fs). For longer pulse duration (several hundred of femtoseconds) a $I^{1/2}$ scaling law is observed with Nd:glass

Photonics North 2011, edited by Raman Kashyap, Michel Têtu, Rafael N. Kleiman, Proc. of SPIE Vol. 8007, 80070L · © 2011 SPIE · CCC code: 0277-786X/11/$18 · doi: 10.1117/12.905822

laser system facilities that reach higher energy level but have lower repetition rate. The maximum proton energy achieved so far with INRS 100 TW class laser system fits correctly in the previously published trends. We obtained 12 MeV for $4\times10^{19}$ W/cm$^2$ intensity on target whereas the maximum proton energy generated with a similar laser system achieved so far is 17 MeV with $10^{21}$ W/cm$^2$ and 30 fs laser pulse duration [6].

A major parameter to control the laser plasma generation is the laser pulse contrast ratio: the presence of a pedestal before the main pulse peak can produce a pre-plasma on the target surfaces and thus modify the interaction parameters. Moreover, reducing the target thickness allows reinforcing electrons recirculation which can increase the accelerating field. Using ultra-thin targets below 100 nm can dramatically be affected by a pre-pulse. Using a peak intensity of $10^{19}$ W/cm$^2$ one needs at least 10 orders of magnitude of laser pulse contrast ratio. Indeed, a pre-pulse of only $10^9$ W/cm$^2$ can significantly change the x-ray emission conversion efficiency [7]. A clear example of the pre-pulse effect on proton emission has been given by Ceccotti et al. [8]. Using a standard Ti:Sapphire $10^6$ contrast ratio, they show that proton emission occurs only on the rear side of the target for a limited range of thicknesses centered close to 20 µm. When a double plasma mirror is used to enhance the contrast ratio by 4 orders of magnitude the proton emission occurs almost symmetrically on both sides of the target for a large thickness range.

Another interest of laser plasma interaction with ultra-thin foil is the possibility to deposit energy in the entire laser absorption depth before any expansion thus enabling target isochoric heating. With a target thickness of 30 or 15 nm the laser pulse should interact in volume and enable to reach very high temperature while the target is still at solid density. The resulting cooling of the target will then be ultra-fast and potential X-ray emission should be ultrashort.

The objective of experiments realized with INRS facility is to study the acceleration mechanism using ultra thin foil target to take advantage of the laser high contrast ratio. In this proceeding we study the maximum proton energy obtained as a function of the target thickness on the front and rear side of the target. Using direct imaging and interferometry measurement we inferred information on plasma expansion. A simple calculation allows us to retrieve the initial electron temperature and a characteristic expansion time which is an indication of isochoric heating of ultra-thin foil at high temperature and of a high cooling rate.

## 2. EXPERIMENTAL SET-UP

The ALLS 100 TW class laser system is described in reference 9. It delivers on target, after compression, 3 J with 30 fs pulse duration at 10 Hz pulse repetition rate and 800 nm wavelength. A detailed characterization of the laser pulse contrast can be found in reference 10. In the present configuration, no extra saturable absorber is used after the regenerative amplifier, but a plasma mirror has been inserted inside the interaction chamber to enhance the laser pulse contrast ratio including the steepness of its rising edge. The laser pulse contrast ratio before the plasma mirror in the nanosecond range is close to $10^8$ in intensity. In the picosecond range the laser pulse contrast ratio is $10^8$-$10^9$ up to 20 ps before the main pulse. The plasma mirror consists of a glass mirror with an anti-reflection coating inserted 7 mm away from the target to reach an energy density on the plasma mirror surface of 100 J/cm$^2$. The laser beam is incident at 45° incidence angle both on the plasma mirror and the target. The laser polarization is linear and parallel to the incidence plane. The plasma mirror reflectivity is 60%. Using a 27 cm focal length off axis parabola (f/3), a 5 µm focal spot (FWHM) is achieved with 30% of the total energy contained within an area limited by the ½ radius. This leads to a peak intensity on target of $4\times10^{19}$ W/cm$^2$.

The experimental set-up has been described in reference 11. Two sets of targets are used: Al foils with thicknesses ranging from 1 µm up to 90 µm and $Si_3N_4$ membranes with thicknesses of respectively 15 and 30 nm. The target reflectivity is measured using a Spectralon, a polymer with high reflectance and a Lambertian behavior, located along the laser specular reflection. An imaging system with high magnification (×40) is used at full energy to monitor the focus of the laser main beam and check its energy distribution and any eventual transmitted energy through the target. The reflectivity of the target is measured to be close to 60% and no transmitted energy through the target is detected even for the thinnest foil used here (15 nm). In this experimental set, the results were obtained using 1.5 J incident on the plasma mirror. The proton spectra on both sides of the target are measured with identical time of flight (TOF) spectrometers.

A laser probe beam (40 fs, 2 mJ) propagating along the target surface is used to image the plasma expansion on both of its sides. A change of the electron density is related to a change of the optical index which results in intensity modulation of the obtained image. This measurement is not a proper shadowgraph measurement, as both refracted and direct beams are detected, and only the qualitative behavior can be retrieved. More quantitative informations about the

plasma expansion process can be obtained using a folded-wave interferometer based on a Michelson geometry with the laser probe [12]. This interferometer is positioned outside the interaction chamber, along the laser probe path, after this last one has gone through the target interaction area. Assuming a cylindrical symmetry for the plasma expansion, the electron density and the length over which the electron density vary can be retrieved for any time delay between the laser probe and the main laser beam.

## 3. RESULTS AND DISCUSSION

### 3.1 Comparison of the proton emission on the front and rear side of the target

The laser pulse contrast ratio is high enough to observe TNSA proton acceleration on both sides of the target. Figure 1 shows pictures of the plasma expansion of Al target foils as a function of the target thickness for a 1 ns time delay between the laser probe and the main laser beam. The expansion on the front side of the target is similar for all the studied thicknesses. On the rear side of the target, when the target thickness is reduced the plasma expansion length becomes higher. For a thickness larger than 30 µm the plasma rear side expansion is very tenuous and almost not visible on the pictures. For a 6.5 µm thickness, the plasma is pinched close to the target surface probably due to the presence of a high magnetic field generated by electrons currents. For a 1 µm thickness, the plasma expansion is similar on both sides of the target. The maximum proton energy as a function of the target thickness is shown on Fig. 2. The highest proton energy produced is obtained for the thinnest foil with a proton energy close to 4.5 MeV generated on the front side of the target. The general trend is a smooth increase of the maximum proton energy when the target thickness is reduced. This is in agreement with the fact that reducing the target thickness allows reinforcing electrons recirculation and increasing the accelerating field. It can be observed that for target thickness greater than 30 µm no proton acceleration is detected on the rear side of the target (the diagnostic sensitivity is limited to 600 keV due to the filter thickness used in front of the scintillator detector).

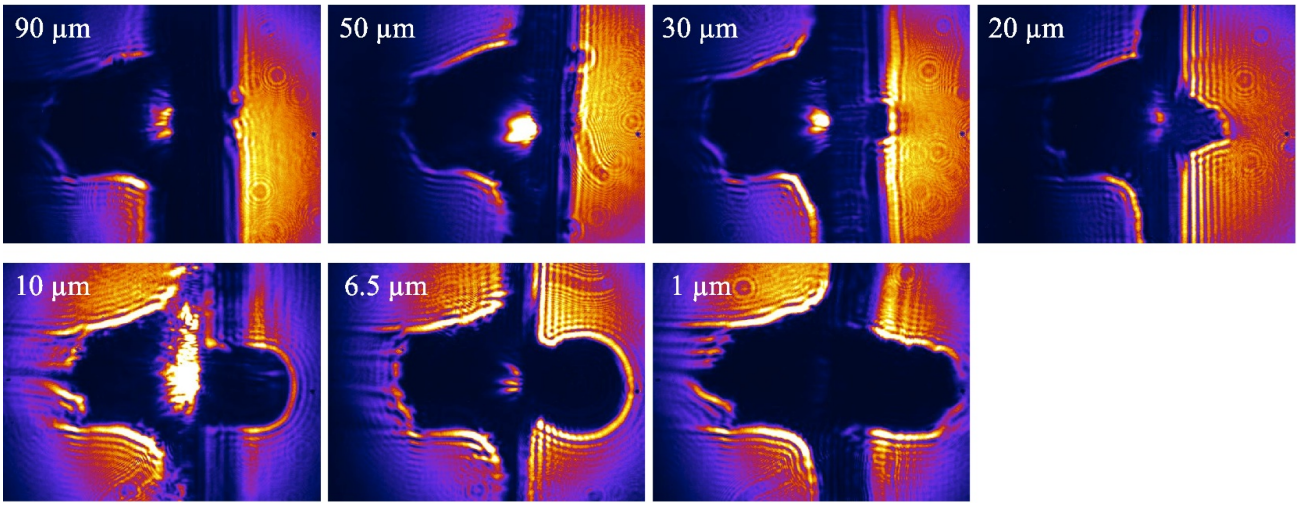


Figure 1: Pictures showing the plasma expansion of Al foils targets with thicknesses ranging from 90 µm down to 1 µm. The target front side is the left of each picture. The time delay between the laser probe and the main laser beam is 1 ns.

To further enhance the acceleration process we used thinner targets, and to do so we had to work with $Si_3N_4$ ultra-thin membranes of respectively 30 and 15 nm thicknesses. The plasma expansion on the front side of the target at 31.3 ps delay between the laser probe and the main laser beam is shown on figure 3. The plasma expansion is masked on the target rear side by the Si frame over which the membrane is built, but for this thickness we expect the plasma expansion process to be similar on each side. The maximum proton energies are 11 MeV and 7.7 MeV respectively on the front and rear side of the 30 nm target. The maximum proton energies are 10.6 MeV and 7.5 MeV respectively on the front and

rear side of the 15 nm target. In this configuration, the laser pulse contrast ratio is high enough to get higher proton maximum energies when reducing the target thickness. For all the studied thicknesses, the maximum proton energy originating from the front side of the target is higher compared to the rear side of the target whereas for thinner targets thicknesses the mechanism is expected to be symmetric. This could be due to a measurement artifact as we didn't check the spatial distribution of the proton emission and the measurement of the proton spectra was achieved normal to the target surface.

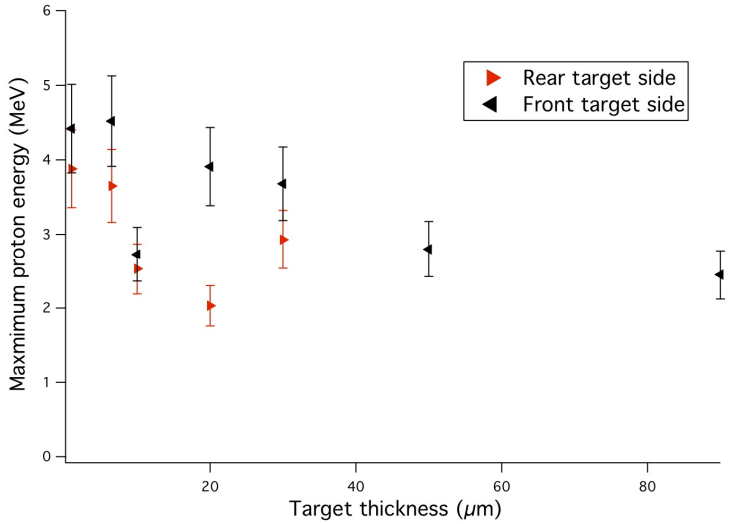


Figure 2: Maximum proton energy as a function of the target thickness. These measurements correspond to the pictures set shown on Fig. 1. For a thickness larger than 30 µm no proton emission is detected on the rear side of the target.

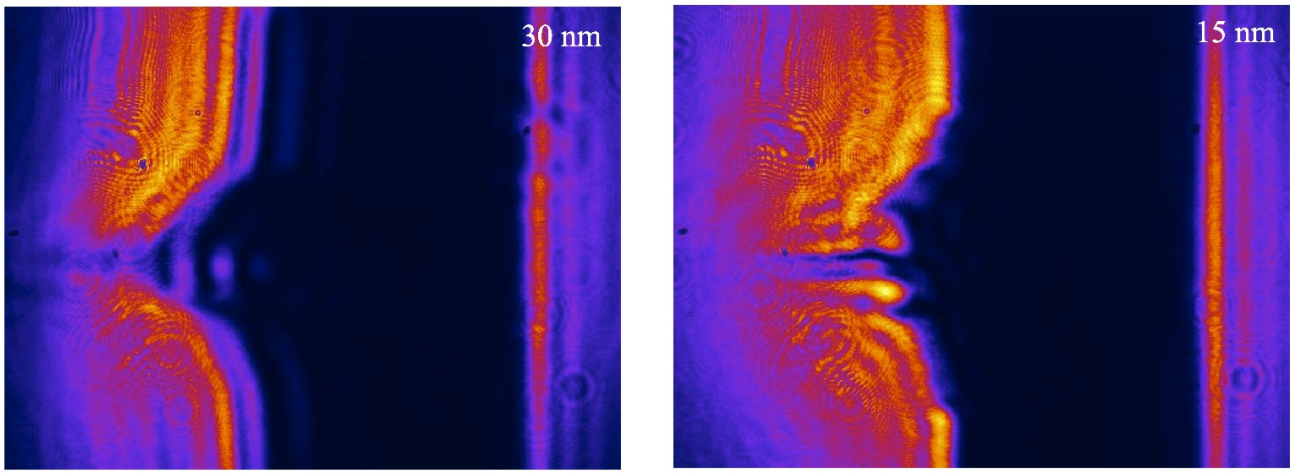


Figure 3: Pictures showing the plasma expansion of Si3N4 membranes targets with thicknesses of 30 and 15 nm. The target front side is the left of each picture. Only the plasma expansion on the front side of the target can be seen as the membrane is fabricated over a Si frame 200 µm thick which hides the plasma expansion on the rear side of the target over this length. The time delay between the laser probe and the main laser beam is 31.3 ps.

The maximum proton energy for thick Al targets is 2.5-3 MeV which is four times lower compared to the maximum proton energy achieved with the membranes targets. For future application development, the experimental set-up could be simplified a lot using a thick target combined with a high contrast laser pulse, which would be suitable for high repetition rate measurements but at the cost of a maximum proton energy reduction.

### 3.2 Correlation of the expansion velocity deduced from direct imaging and interferometry

We can determine an expansion length *Le* and velocity V*e* along the axis normal to the target surface using the plasma edge position corresponding to a strong reduction of the laser probe transmitted light from the pictures presented in Fig. 1 and 3. To determine the electron density to which corresponds this expansion edge, we used interferogram pictures obtained from the folded-wave interferometer. Figure 4 show the plasma expansion from a $Si_3N_4$ target with two background fringes patterns imaged by two separate CCD cameras and during the same laser shot. We can compare the first image with zero fringes (Fig. 4a), which is similar to the direct imaging, with the second image with nonzero fringes (Fig. 4b). Assuming that the plasma expansion has a cylindrical geometry, we can define a mean electron density corresponding to the lateral distance over which the laser probe light is strongly reduced. Using these assumptions we find a value close to $10^{19}$ $cm^{-3}$ for the mean electron density along the edge of the plasma with a confidence interval of 8-$18\times10^{18}$ $cm^{-3}$.

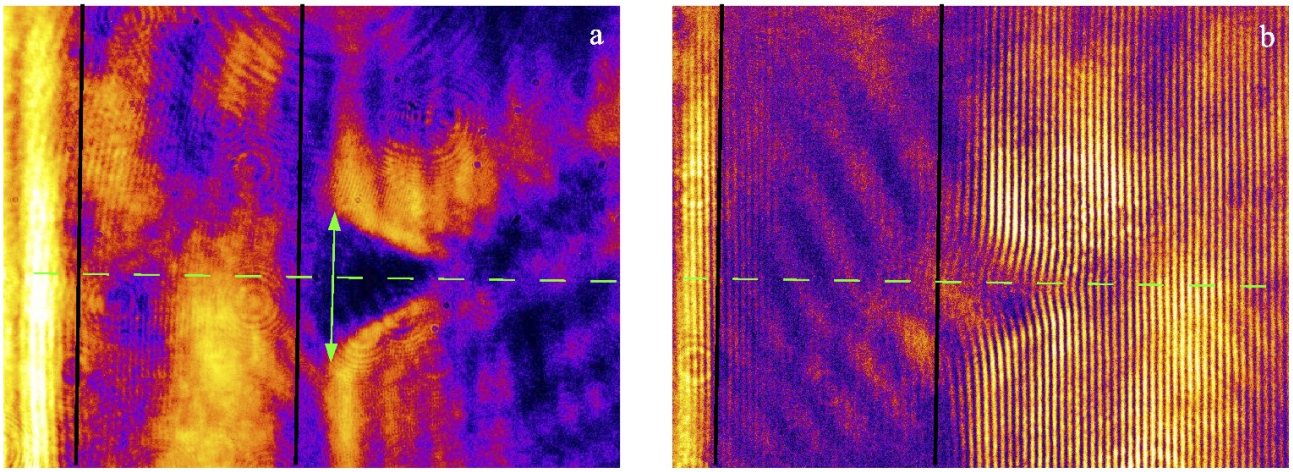


Figure 4: Pictures showing the plasma expansion of a 15 nm $Si_3N_4$ membrane target. The same measurement is shown using a folded wave interferometer:a- zero fringes is used as a reference for direct imaging. The green arrow shows the lateral dimension over which the density is integrated and the green non continuous line correspond to the axis on which the expansion length and speed are determined; b- nonzero fringes are used parallel to the target surface as reference. The target front side is the right of each picture. The black continuous vertical lines show the position of the target.

### 3.3 Study of the plasma expansion velocity

From the pictures obtained on Fig. 1, we can deduce the plasma edge position and calculate *Ve* the plasma velocity for a time delay between the laser probe and the main laser beam of 1 ns. Figure 5 shows the expansion speed as a function of the target thickness corresponding to the measurement set of Fig. 1. The plasma edge velocity is around $1.5\times10^7$ cm/s on the front side of the target. On the rear side, the plasma edge velocity increases for a reduced thickness as the electrons propagation length inside the target is shortened. When we consider the ultra-thin $Si_3N_4$ membranes, the expansion velocities are $3.1\times10^8$ and $3.3\times10^8$ cm/s respectively for the 30 and 15 nm membrane thickness. The time delay between the laser probe and the main laser beam for which these last values are determined is 31.3 ps instead of 1 ns for the Al foils target. To be able to compare the expansion speed at the same time delay, we studied the time evolution of the expansion speed for a 15 nm thick $Si_3N_4$ membrane by changing the time delay of the laser probe compared to the main laser beam.

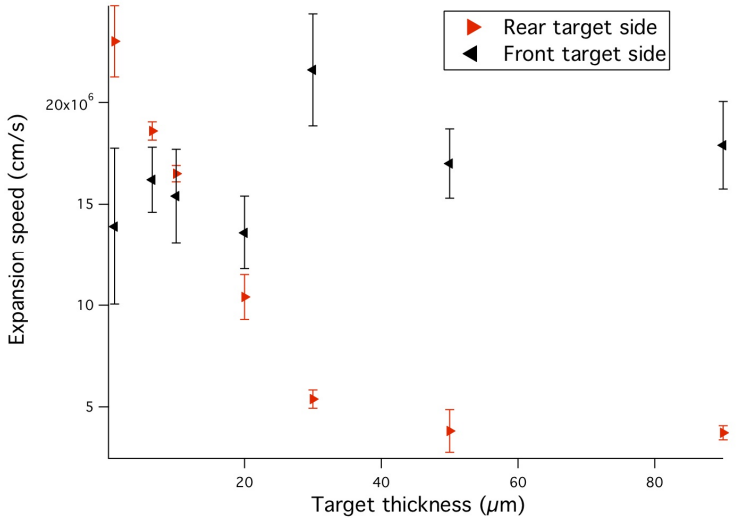


Figure 5: Expansion speed of the plasma edge as a function of the Al target thickness. These measurements correspond to the pictures set shown on Fig. 1.

The plasma expansion length for a 15 nm thick $Si_3N_4$ membrane as a function of the time delay between the laser probe and the main laser beam is shown on figure 6. We fitted the experimental point of Fig. 6 with a power function: $Le = Yo + A \times t^{pow}$ . *Le* is the expansion length and *t* is the time delay. *Yo*, *A* and *pow* are the fitting parameters. We found *pow = 0.12*. The maximum proton energy produced in the case of this study of the plasma expansion as a function of the time delay is reduced compared to the results obtained for figure 3: its value is reduced to 2 MeV instead of 10 MeV. This is explained by a decrease of the focusing quality due to a wavefront degradation.

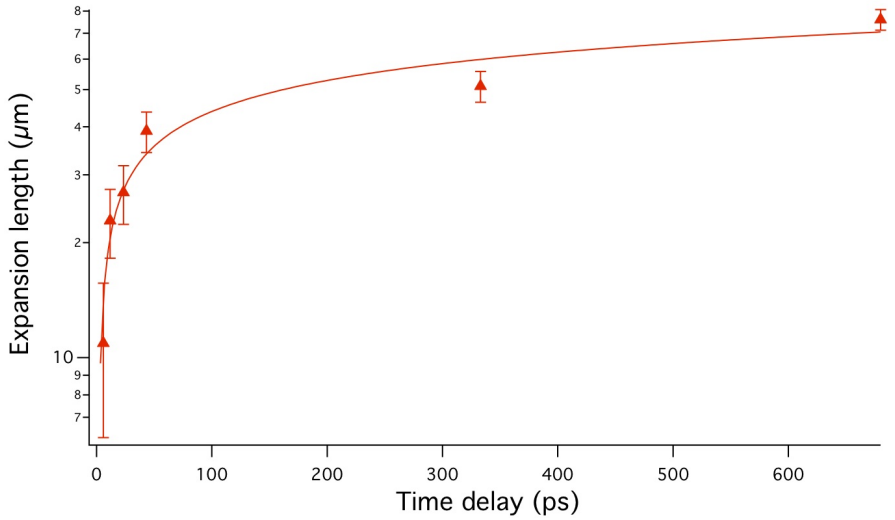


Figure 6: Position of the plasma edge as a function of the time delay between the laser probe and the main laser beam. The target is a 15 nm thick $Si_3N_4$ membranes. The plasma edge position corresponds to an electron density close to $10^{19}$ $cm^{-3}$. The red continuous line corresponds to a fit to a power function.

The expansion speed *Ve* for large delay is close to $1.5\times10^7$ cm/s compared to $10^8$ cm/s for a time delay below 50 ps. This can be interpreted with the existence of a two regime plasma expansion process corresponding to two expansion speeds. The expansion velocity found for the $Si_3N_4$ membranes target from Fig. 3 correspond to the first plasma expansion regime when the time delay is below 50 ps and a high expansion speed is measured ($3\times10^8$ cm/s). In this case, for the higher time delay close to 1 ns, we can approximate the expansion speed to be a few times $10^7$ cm/s similar to what was found for the experimental set with Al targets foil of Fig. 1.

The electron temperature *Te* can be crudely estimated if we know the amount of energy *Ee-* absorbed by each heated electron. The absorbed laser energy *Ea* heats the electrons over a limited volume *Vh* corresponding to the laser absorption depth. The mass of this heated volume can be calculated knowing the target density ρ. The number of heated electrons *Nh* can also be evaluated by making the assumption that the target is totally ionized (we call *Nz* the number of electrons produced from every molecule) $Nh = Vh\times\rho\times Nz\times Na/M$. *Na* is the Avogadro number and *M* the molar mass. The considered absorbed energy is $Ea \sim \rho\times Vh\times Ve^2$.

If we consider a $Si_3N_4$ membrane target, with $Ea = 180$ mJ and an initial expansion speed $Ve = 1\times10^8$ cm/s, then $Vh \sim 10^{-10}$ $cm^3$ and $Nh \sim 5\times10^{11}$ electrons which results in $Te \sim 9$ keV.

Assuming that the laser pulse interacts with a 15 nm thick target on the front side of the target, we can define a characteristic time $\tau = do/Ve$. This corresponds to the time it takes for the interaction thickness to double. The numerical application gives $\tau = 15\times10^{-7}/1.0\times10^8 = 15$ fs.

We will use a more precise model in future works, but the current calculations indicate that the target is heated to very high temperature and the related cooling rate is ultrashort making it of potential interest for isochoric heating.

## ACKNOWLEDGMENTS

The authors would like to thanks the work done by the INRS-EMT and ALLS technical team: Marc Olivier Bussière, Guy Lebrun, Joël Maltais, Carol Morissette, Léonard Pelletier, François Poitras, Pierre-Luc Renault and Claude Sirois. The ALLS facility has been funded by the Canadian Foundation for Innovation (CFI). This work is funded by NSERC, the Canada Research Chair program and by Ministère de l'éducation du Québec.

## REFERENCES

1. R. A. Snavely, M. H. Key, S. P. Hatchett, T. E. Cowan et al., "*Intense High-Energy Proton Beams from Petawatt-Laser Irradiation of Solids*," *Phys. Rev. Lett.* **85**, pp 2945-2948, 2000.
2. E. L. Clark, K. Krushelnick, J. R. Davies, M. Zepf et al., "*Measurements of Energetic Proton Transport through Magnetized Plasma from Intense Laser Interactions with Solids*," *Phys. Rev. Lett.* **84**, pp 670–673, 2000.
3. K. Krushelnick, E. L. Clark, M. Zepf, J. R. Davies et al., "*Energetic proton production from relativistic laser interaction with high density plasmas," Phys. Plasmas* **7**, pp 2055, 2000.
4. S. A. Gaillard, K. A. Flippo, D. C. Gautier, D.T. Offermann et al., "*65+ MeV Protons from Short-Pulse-Laser Micro-Cone-Target Interactions,"* APS DPP, Atlanta, 2009.
5. J Fuchs, "*Accélération de faisceaux d'ions par laser intense ultracourt et applications,"* HDR thesis, LULI UMR 7605 CNRS-CEA-École Polytechnique-Université Paris VI, Palaiseau, 2007.
6. K. Zeil, S. D. Kraft, S. Bock et al., "The scaling of proton energies in ultrashort pulse laser plasma acceleration," *New Journal of Physics.* **12**, pp 045015, 2010.
7. K. B. Wharton, C. D. Boley, A. M. Komashko, A. M. Rubenchik et al., "*Effects of nonionizing prepulses in high-intensity laser-solid interactions*," *Phys. Rev. E* **64**, pp 025401(R), 2001.
8. T. Ceccotti, A. Lévy, H. Popescu, F. Réau et al., "*Proton Acceleration with High-Intensity Ultrahigh-Contrast Laser Pulses," Phys. Rev. Lett.* **99**, 185002, 2007.
9. S. Fourmaux, S. Payeur, A. Alexandrov et al., "Laser beam wavefront correction for ultra high intensities with the 200 TW laser system at the advanced laser light source," Optics Express 16, pp. 11987-11994 (2008).
10. S. Fourmaux, S. Payeur, S. Buffechoux et al., "Pedestal cleaning for high laser pulse contrast ratio with a 100 TW class laser system," Optics Express 19, pp. 8486-8497 (2011).
11. S. Fourmaux, S. Buffechoux et al. "Laser-based proton acceleration experiments at the ALLS facility using a 200 TW high intensity laser system*,"* Proc. SPIE Int. Soc.Opt. Eng. Vol. 7750, 77500W (2010).
12. F. Martin, "Folded-wave interferometer for laser-matter interaction studies*," Applied Optics* **19**, pp. 4230–4232, 1980.